

Anomalous triple gauge boson couplings in ZZ production at the LHC and the role of Z boson polarizations

Rafiqul Rahaman* and Ritesh K. Singh†

Department of Physical Sciences, Indian Institute of Science Education and Research
Kolkata, Mohanpur, 741246, India

Abstract

We study anomalous couplings among neutral gauge bosons in ZZ production at the LHC for $\sqrt{s} = 13$ TeV in 4-lepton final state. We use the cross section and polarization asymmetries of the Z boson to estimate simultaneous limits on anomalous coupling using Markov-Chain-Monte-Carlo (MCMC) method for luminosities 35.9 fb^{-1} , 150 fb^{-1} , 300 fb^{-1} and 1000 fb^{-1} . The CP -even polarization asymmetry $A_{x^2-y^2}$ is sensitive mainly to the CP -odd couplings $f_4^{Z/\gamma}$ (quadratically) providing a probe to identify CP -odd nature of interaction at the LHC. We find that the polarization asymmetries significantly improve the estimation of anomalous couplings should a deviation from the Standard Model (SM) be observed.

1 Introduction

The Standard Model (SM) of particle physics is a highly successful theory in explaining most of the phenomena in Nature. The last milestone of the SM, the Higgs boson discovered [1] at the Large Hadron Collider (LHC) confirmed the Electro Weak Symmetry Breaking (EWSB), which is still not fully understood. To understand this, one needs a precise measurement of the Higgs self couplings, Higgs to gauge boson couplings and gauge boson self couplings. Anomalous triple gauge boson couplings (aTGC) can play an important role in understanding the EWSB mechanism. Absence of neutral aTGC at the LHC will provide support to the EWSB, while the presence of it will indicate new physics possibility needed to explain many phenomena such as CP -odd, Baryogenesis, dark matter, etc. The ZZ and $Z\gamma$ production are the two main processes where one can study the neutral aTGC. The neutral aTGC can be obtained by adding higher dimension effective operators to the SM [2–4]. The neutral aTGC start appearing at dimension-8 onward and hence their effect is expected to be very small at low energy. Alternatively, one can also parametrize the neutral aTGC with dimension-6 (and 8) form factors in a model-independent way [5]. A Lagrangian for the parametrization discussed in Ref. [5] consisting terms

*rr13rs033@iiserkol.ac.in

†ritesh.singh@iiserkol.ac.in

up to dimension-6 is given by [6]

$$\mathcal{L}_{ZZV} = \frac{e}{M_Z^2} \left[- \left[f_4^\gamma \left(\partial_\mu F^{\mu\beta} \right) + f_4^Z \left(\partial_\mu Z^{\mu\beta} \right) \right] Z_\alpha (\partial^\alpha Z_\beta) + \left[f_5^\gamma (\partial^\sigma F_{\sigma\mu}) + f_5^Z (\partial^\sigma Z_{\sigma\mu}) \right] \tilde{Z}^{\mu\beta} Z_\beta \right. \\ \left. - \left[h_1^\gamma (\partial^\sigma F_{\sigma\mu}) + h_1^Z (\partial^\sigma Z_{\sigma\mu}) \right] Z_\beta F^{\mu\beta} - \left[h_3^\gamma (\partial_\sigma F^{\sigma\rho}) + h_3^Z (\partial_\sigma Z^{\sigma\rho}) \right] Z^\alpha \tilde{F}_{\rho\alpha} \right], \quad (1)$$

where $\tilde{Z}_{\mu\nu} = 1/2\epsilon_{\mu\nu\rho\sigma}Z^{\rho\sigma}$ ($\epsilon^{0123} = +1$) with $Z_{\mu\nu} = \partial_\mu Z_\nu - \partial_\nu Z_\mu$ and similarly for the photon tensor $F_{\mu\nu}$. Among these anomalous couplings f_4^V, h_1^V ($V = Z, \gamma$) are CP -odd in nature and f_5^V, h_3^V are CP -even. The couplings f^V appear only in the ZZ production process, while h^V appear in the $Z\gamma$ production process. The anomalous neutral triple gauge boson couplings in Eq. (1) have been widely studied in the literature [6–27] for various colliders: in e^+e^- collider [7, 9, 17–19, 21–25], $e\gamma$ collider [10, 15, 16], $\gamma\gamma$ collider [20], hadron collider [8, 12, 14, 26, 27] and both e^+e^- and hadron collider [6, 11, 13].

On the experimental side, the anomalous Lagrangian in Eq. (1) have been explored at the LEP [28–32], the Tevatron [33–35] and the LHC [36–42]. The tightest 95 % C.L. limits on anomalous couplings are obtained in ZZ production at the LHC [42] running at $\sqrt{s} = 13$ TeV with $\mathcal{L} = 35.9 \text{ fb}^{-1}$ and they are given by

$$\begin{aligned} -0.0012 < f_4^Z < 0.0010, \quad -0.0010 < f_5^Z < 0.0013, \\ -0.0012 < f_4^\gamma < 0.0013, \quad -0.0012 < f_5^\gamma < 0.0013, \end{aligned} \quad (2)$$

obtained by varying one parameter at a time and using only the cross section as observable. We note that these ranges of couplings do not violate unitarity bound up to an energy scale of 10 TeV. Whereas a size as large as $\mathcal{O}(\pm 0.1)$ of the couplings can be allowed if the unitarity violation is assumed to take place at the energy scale of 3 TeV, a typical energy range explored by the current 13 TeV LHC.

The tensorial structure for some of these anomalous couplings can be generated at higher order loop within the framework of a renormalizable theory. For example, a fermionic triangular diagram can generate CP -even couplings in the SM, some simplified fermionic model [43], the Minimal Supersymmetric SM (MSSM) [44, 45] and Little Higgs model [46]. On the other hand, CP -odd couplings can be generated at 2 loop in the MSSM [44]. A CP -violating ZZZ vertex has been studied in 2HDM in Ref. [43, 47, 48]. Besides this, the non-commutative extension of the SM (NCSM) [49] can also provide these anomalous coupling structures. We note that in the EFT framework these trilinear couplings can be obtained at dimension-8 operator which also contribute to quartic gauge boson couplings $WWVV, ZZZ\gamma, ZZ\gamma\gamma$ which appear in triple gauge boson production [50, 51] and vector boson scattering [52], for example. A complete study of these operators will require one to include all these processes involving triple gauge boson couplings as well as quartic gauge boson couplings. In the effective form factor approach as we study in this paper, however, the triple and the quartic gauge boson couplings are independent of each other and can be studied separately.

Here we study anomalous triple gauge boson couplings in the neutral sector in the framework of the model independent Lagrangian in Eq. (1) using polarization observables of Z boson [22, 53, 54] in ZZ pair production at the LHC. The polarization asymmetries of Z and W have been used earlier to study the anomalous couplings in $ZZ/Z\gamma$ production at e^+e^- collider [22, 23], in W^+W^- production at e^+e^- collider [55, 56]. The polarization asymmetries have also been used to study Higgs-gauge boson interaction [57, 58], for dark matter studies [59], for testing the top

quark mass structure [60, 61], for studies of special interactions of massive particles [62, 63], and for studies of dark matter and heavy resonance [64]. The LHC being a symmetric collider, many polarization out of 8 polarization of Z boson cancels out, however, three of them are non zero, which are discussed in section 2.

The leading order (LO) result of the ZZ pair production cross section is way below the result measured at the LHC [41, 42]. However, the existing next-to-next-to-leading order (NNLO) [65, 66] results are comparable with the measured values at CMS [42] and ATLAS [41]. We, however, obtain the cross section at next-to-leading order (NLO) in the SM and in aTGC using MADGRAPH5_aMC@NLO [67] and have used the SM k -factor to match to the NNLO value. The details of these calculations are described in section 3.

The rest of the paper is organized as follows. In section 2 we give a brief overview of the polarization observables of the Z boson. In section 3 we discuss LO, NLO and NNLO result for ZZ production including aTGC and various background processes. In section 4 we study the sensitivity of observables to couplings and obtain one parameter as well as simultaneous limits on the couplings. We also study a benchmark aTGC and investigate how polarization asymmetries can improve the estimation of anomalous couplings. We conclude in section 5.

2 Polarization observables of Z

The normalized production density matrix of a spin-1 particle (here Z) can be written as [53, 68]

$$\rho(\lambda, \lambda') = \frac{1}{3} \left[I_{3 \times 3} + \frac{3}{2} \vec{p} \cdot \vec{S} + \sqrt{\frac{3}{2}} T_{ij} (S_i S_j + S_j S_i) \right], \quad (3)$$

where $\vec{S} = \{S_x, S_y, S_z\}$ are the spin basis, $\vec{p} = \{p_x, p_y, p_z\}$ are the vector polarizations, T_{ij} (2^{nd} -rank symmetric traceless tensor) are tensor polarizations and $(\lambda, \lambda') \in \{+1, 0, -1\}$ are helicities of the particle. After expansion Eq. (3) can be rewritten as*

$$\rho(\lambda, \lambda') = \begin{bmatrix} \frac{1}{3} + \frac{p_z}{2} + \frac{T_{zz}}{\sqrt{6}} & \frac{p_x - ip_y}{2\sqrt{2}} + \frac{T_{xz} - iT_{yz}}{\sqrt{3}} & \frac{T_{xx} - T_{yy} - 2iT_{xy}}{\sqrt{6}} \\ \frac{p_x + ip_y}{2\sqrt{2}} + \frac{T_{xz} + iT_{yz}}{\sqrt{3}} & \frac{1}{3} - \frac{2T_{zz}}{\sqrt{6}} & \frac{p_x - ip_y}{2\sqrt{2}} - \frac{T_{xz} - iT_{yz}}{\sqrt{3}} \\ \frac{T_{xx} - T_{yy} + 2iT_{xy}}{\sqrt{6}} & \frac{p_x + ip_y}{2\sqrt{2}} - \frac{T_{xz} + iT_{yz}}{\sqrt{3}} & \frac{1}{3} - \frac{p_z}{2} + \frac{T_{zz}}{\sqrt{6}} \end{bmatrix}. \quad (4)$$

The Eq. (4) is called a polarization density matrix of a spin-1 particle. The 8 independent polarizations p_x, p_y, p_z and $T_{xy}, T_{xz}, T_{yz}, T_{xx} - T_{yy}$ and T_{zz} can be calculated from a production density matrix of the particle in any production process [23, 54]. The laboratory (Lab) frame and centre-of-mass frame (CM) being different at the LHC, the polarization calculated at CM frame will not be the same as the polarization at Lab frame, unlike the total cross section. The production density matrix receives a total rotation leaving the trace invariant when boosted from CM to Lab frame. These leads to the polarization parameters p_i and T_{ij} getting transformed as [68]

$$\begin{aligned} p_i^{Lab} &= \sum_j R_{ij}^Y(\omega) p_j^{CM}, \\ T_{ij}^{Lab} &= \sum_{k,l} R_{ik}^Y(\omega) R_{jl}^Y(\omega) T_{kl}^{CM}, \end{aligned} \quad (5)$$

*The choice of polarization vector is used to be $\epsilon_Z(\lambda = \pm 1) = \frac{1}{\sqrt{2}}\{0, \mp 1, -i, 0\}$.

where

$$\begin{aligned}\cos \omega &= \cos \theta_{CM} \cos \theta_{Lab} + \gamma_{CM} \sin \theta_{CM} \sin \theta_{Lab}, \\ \sin \omega &= \frac{M}{E_{CM}} (\sin \theta_{CM} \cos \theta_{Lab} - \gamma_{CM} \cos \theta_{CM} \sin \theta_{Lab}),\end{aligned}\quad (6)$$

R_{ij}^Y is the usual rotational matrix w.r.t. y -direction, θ is the polar angle of the particle w.r.t. z -direction, M is the rest mass, E_{CM} is the energy in CM frame and $\gamma_{CM} = 1/\sqrt{1 - \beta_{CM}^2}$ with β_{CM} being boost of the CM frame[†].

Combining the normalized production matrix in Eq. (4) with normalized decay density matrix of the particle to a pair of fermion f , the normalised differential cross section would be [53]

$$\begin{aligned}\frac{1}{\sigma} \frac{d\sigma}{d\Omega_f} &= \frac{3}{8\pi} \left[\left(\frac{2}{3} - (1 - 3\delta) \frac{T_{zz}}{\sqrt{6}} \right) + \alpha p_z \cos \theta_f + \sqrt{\frac{3}{2}} (1 - 3\delta) T_{zz} \cos^2 \theta_f \right. \\ &+ \left(\alpha p_x + 2\sqrt{\frac{2}{3}} (1 - 3\delta) T_{xz} \cos \theta_f \right) \sin \theta_f \cos \phi_f \\ &+ \left(\alpha p_y + 2\sqrt{\frac{2}{3}} (1 - 3\delta) T_{yz} \cos \theta_f \right) \sin \theta_f \sin \phi_f \\ &+ (1 - 3\delta) \left(\frac{T_{xx} - T_{yy}}{\sqrt{6}} \right) \sin^2 \theta_f \cos(2\phi_f) \\ &\left. + \sqrt{\frac{2}{3}} (1 - 3\delta) T_{xy} \sin^2 \theta_f \sin(2\phi_f) \right].\end{aligned}\quad (7)$$

Here θ_f , ϕ_f are the polar and the azimuthal orientation of the fermion f , in the rest frame of the particle (Z) with its would be momentum along the z -direction. For massless final state fermions, we have $\delta = 0$ and $\alpha = (R_f^2 - L_f^2)/(R_f^2 + L_f^2)$ where the $Zf\bar{f}$ coupling is of the type $\gamma^\mu (L_f P_L + R_f P_R)$. The polarizations p_i and T_{ij} are calculable from asymmetries constructed from the decay angular information of lepton using Eq. (7). For example, $T_{xx} - T_{yy}$ can be calculated from the asymmetry $A_{x^2-y^2}$ as

$$\begin{aligned}A_{x^2-y^2} &= \frac{1}{\sigma} \left[\left(\int_{-\pi/4}^{\pi/4} \frac{d\sigma}{d\phi} d\phi + \int_{3\pi/4}^{5\pi/4} \frac{d\sigma}{d\phi} d\phi \right) - \left(\int_{\pi/4}^{3\pi/4} \frac{d\sigma}{d\phi} d\phi + \int_{5\pi/4}^{7\pi/4} \frac{d\sigma}{d\phi} d\phi \right) \right] \\ &\equiv \frac{\sigma(\cos 2\phi > 0) - \sigma(\cos 2\phi < 0)}{\sigma(\cos 2\phi > 0) + \sigma(\cos 2\phi < 0)} \\ &= \frac{1}{\pi} \sqrt{\frac{2}{3}} (1 - 3\delta) (T_{xx} - T_{yy}).\end{aligned}\quad (8)$$

Likewise one can construct asymmetries corresponding to each of the polarizations p_i and T_{ij} , see Ref. [22] for details.

The LHC being a symmetric collider, most of the polarization of Z in ZZ pair production are either zero or close to zero except the polarization T_{xz} , $T_{xx} - T_{yy}$, and T_{zz} . To enhance the significance further we redefine the asymmetry corresponding to T_{xz} as (see Ref. [23])

$$\tilde{A}_{xz} \equiv \frac{1}{\sigma} \left(\sigma(c_{\theta_Z} \times c_{\theta_f} c_{\phi_f} > 0) - \sigma(c_{\theta_Z} \times c_{\theta_f} c_{\phi_f} < 0) \right),\quad (9)$$

where c_{θ_Z} is the cosine of Z boson polar angle in the lab frame. To get the momentum direction of Z boson, one needs a reference axis (z -axis), but we can not assign a direction at the LHC

[†]These properties has been used in Ref. [69, 70].

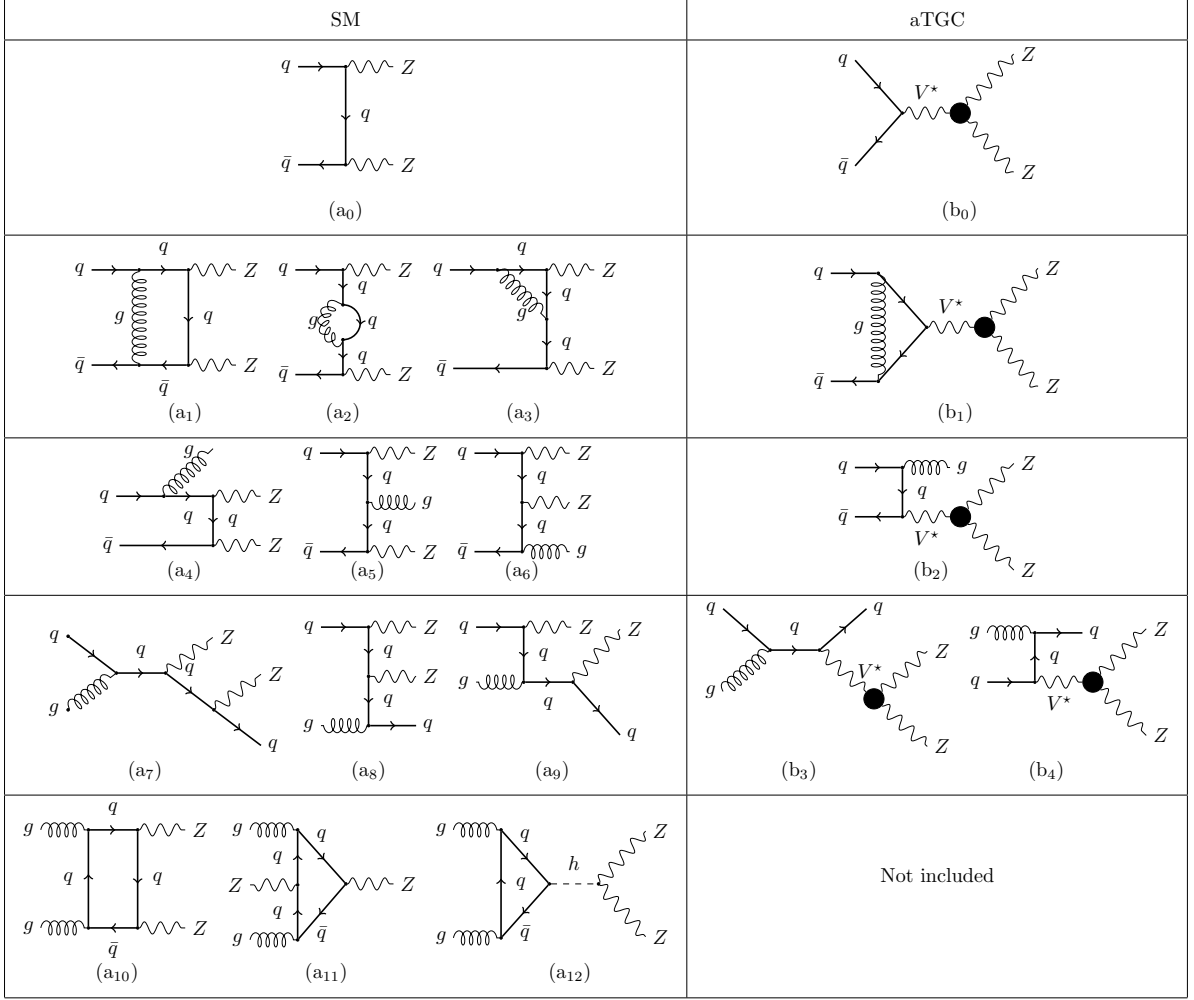


Figure 1: Representative Feynman diagrams for ZZ pair production at the LHC in the SM ($q\bar{q}$ and gg initiated) as well as in aTGC ($q\bar{q}$ initiated) at tree level together with NLO in QCD.

because it is a symmetric collider. So we consider the direction of boost of the $4l$ final state to be the proxy for reference z -axis. In $q\bar{q}$ fusion, the quark is supposed to have larger momentum than the anti-quark at the LHC, thus above proxy statistically stands for the direction of the quark and c_{θ_Z} is measured w.r.t. the boost.

3 Signal and background

We are interested in studying anomalous triple gauge boson couplings in ZZ pair production at the LHC. The tree level standard model contribution to this process comes from the representative diagram (a₀) in Fig. 1, while the tree level aTGC contribution is shown in the diagram (b₀). Needless to say, the tree level cross section in the SM is way below the measured cross section at the LHC, because QCD corrections are very high in this process. In the SM, at NLO ($\mathcal{O}(\alpha_s)$), virtual contributions come from the representative diagrams (a₁–a₃) and real contributions come from (a₄–a₉) in the $q\bar{q}$ initiated sub-process. The gg initiated sub-process appears at 1-loop level, the diagrams (a₁₀–a₁₂), and contributes at $\mathcal{O}(\alpha_s^2)$. The LO, NLO and NNLO results from theoretical calculation available in literature [65, 66] for ZZ production cross section at $\sqrt{s} = 13$

Table 1: The theoretical estimates available in literature and experimental measurements of the ZZ production cross section at $\sqrt{s} = 13$ TeV at the LHC. The uncertainties in the theoretical estimates come from scale variation.

Ref.	σ_{LO} [pb]	σ_{NLO} [pb]	σ_{NNLO} [pb]
Ref. [65]	$9.890^{+4.9\%}_{-6.1\%}$	$14.51^{+3.0\%}_{-2.4\%}$	$16.92^{+3.2\%}_{-2.6\%}$
Ref. [66]	$9.887^{+4.9\%}_{-6.1\%}$	$14.51^{+3.0\%}_{-2.4\%}$	$16.91^{+3.2\%}_{-2.4\%}$
CMS [42]	$17.2 \pm 0.5(\text{stat.}) \pm 0.7(\text{syst.}) \pm 0.4(\text{lumi.})$		
ATLAS [41]	$17.3 \pm 0.6(\text{stat.}) \pm 0.5(\text{syst.}) \pm 0.6(\text{lumi.})$		

TeV for a pp collider are listed in Table 1. The recent experimental measurement from CMS [42] and ATLAS [41] are also shown for comparison. The cross section at NLO receives as much as ~ 46 % correction over LO and further the NNLO cross section receives ~ 16 % correction over the NLO result. At NNLO the $q\bar{q}$ sub-process receives 10 % correction [66] over NLO and the gg initiated $\mathcal{O}(\alpha_s^3)$ sub-process receives 70 % correction [71] over it's $\mathcal{O}(\alpha_s^2)$ result. The LO and NLO results obtained in MADGRAPH5_aMC@NLO v2.6.2 with pdf (parton-distribution-function) sets NNPDF23 are

$$\begin{aligned}
\sigma_{\mathcal{O}(\alpha_s^0)}^{q\bar{q} \rightarrow ZZ} &= 9.341^{+4.3\%}_{-5.3\%} \text{ pb}, \\
\sigma_{\mathcal{O}(\alpha_s)}^{q\bar{q} \rightarrow ZZ} &= 13.65^{+3.2\%}_{-3.6\%} \text{ pb}, \\
\sigma_{\mathcal{O}(\alpha_s^2)}^{gg \rightarrow ZZ} &= 1.142^{+24.5\%}_{-18.7\%} \text{ pb}, \\
\sigma_{\text{mixed}_1}^{q\bar{q}+gg \rightarrow ZZ} &= \sigma_{\mathcal{O}(\alpha_s)}^{q\bar{q} \rightarrow ZZ} + \sigma_{\mathcal{O}(\alpha_s^2)}^{gg \rightarrow ZZ} \\
&= 14.79^{+4.8\%}_{-4.7\%} \text{ pb}.
\end{aligned} \tag{10}$$

The errors in the subscript and superscript on the cross section are the uncertainty from scale variation. The total cross section combining the $q\bar{q}$ sub-process at $\mathcal{O}(\alpha_s^2)$ with gg at $\mathcal{O}(\alpha_s^3)$ is given by

$$\begin{aligned}
\sigma_{\text{mixed}_2}^{q\bar{q}+gg \rightarrow ZZ} &= \underbrace{\sigma_{\mathcal{O}(\alpha_s)}^{q\bar{q} \rightarrow ZZ} \times 1.1}_{\mathcal{O}(\alpha_s^2)} + \underbrace{\sigma_{\mathcal{O}(\alpha_s^2)}^{gg \rightarrow ZZ} \times 1.7}_{\mathcal{O}(\alpha_s^3)} \\
&= 16.96^{+5.6\%}_{-5.3\%} \text{ pb}.
\end{aligned} \tag{11}$$

The aTGC has also a substantial NLO QCD correction and they come from the diagram (b₂) at 1 loop level and from (b₂–b₄) as the real radiative process. The aTGC effect is not included in the gg process where the aTGC may come from a similar diagram with $h \rightarrow ZZ$ in Fig. 1(a₁₂) but h replaced with a Z . As an example of NLO QCD correction of aTGC in this process, we obtain cross section at $\sqrt{s} = 13$ TeV with all couplings $f_i^V = 0.001$. The cross section for only aTGC part, $(\sigma^{\text{aTGC}} - \sigma^{\text{SM}})$ at LO and NLO are 71.82 fb (0.77 %) and 99.94 fb (0.73 %), respectively. Thus NLO result comes with a substantial amount (~ 39 %) of QCD correction over LO at this given aTGC point.

The signal consists of $4l$ ($2e2\mu/4e/4\mu$) final state which includes ZZ , $Z\gamma^*$, and $\gamma^*\gamma^*$ processes. The signal events are generated in MADGRAPH5_aMC@NLO

with pdf sets NNPDF23 in the SM as well as in the aTGC as $pp \rightarrow VV \rightarrow 2e2\mu$ ($V = Z/\gamma^*$) at NLO in QCD in $q\bar{q}$, qg as well as in 1-loop gg initiated process with the following basic cuts (in accordance with Ref. [42]),

- $p_T^l > 10$ GeV, hardest $p_T^l > 20$ GeV, and second hardest $p_T^l > 12$ GeV,
- $|\eta_e| < 2.5$, $|\eta_\mu| < 2.4$,
- $\Delta R(e, \mu) > 0.05$, $\Delta R(l^+, l^-) > 0.02$.

To select the ZZ final state from the above generated signal we further put a constraint on invariant mass of same flavoured oppositely charged leptons pair with

- $60 \text{ GeV} < M_{l+l^-} < 120 \text{ GeV}$.

The $2e2\mu$ cross section up to a factor of two is used as the proxy for the $4l$ cross section for the ease of event generation and related handling.

The background event consisting $t\bar{t}Z$ and WWZ with leptonic decay are generated at LO in MADGRAPH5_aMC@NLO with NNPDF23 with the same sets of cuts as applied to the signal and their cross section is matched to NLO in QCD with a k -factor of 1.4. This k -factor estimation was done at the production level. We have estimated the total cross section of the signal in the SM to be

$$\begin{aligned}\sigma(pp \rightarrow ZZ \rightarrow 4l)_{\mathcal{O}(\alpha_s)}^{q\bar{q}} &= 28.39 \text{ fb}, \\ \sigma(pp \rightarrow ZZ \rightarrow 4l)_{\mathcal{O}(\alpha_s^2)}^{gg} &= 1.452 \text{ fb}, \\ \sigma(pp \rightarrow ZZ \rightarrow 4l)_{mixed_1}^{q\bar{q}+gg} &= 29.85 \text{ fb}, \\ \sigma(pp \rightarrow ZZ \rightarrow 4l)_{mixed_2}^{q\bar{q}+gg} &= 33.70 \text{ fb}.\end{aligned}\tag{12}$$

The background cross section at NLO is estimated to be

$$\sigma(pp \rightarrow t\bar{t}Z + WWZ \rightarrow 4l + \cancel{E}_T)_{NLO} = 0.020 \text{ fb}.\tag{13}$$

The values of various parameters used for the generation of signal and background are

- $M_Z = 91.1876 \text{ GeV}$, $M_H = 125.0 \text{ GeV}$,
- $G_F = 1.16639 \times 10^{-5} \text{ GeV}^{-2}$, $\alpha_{em} = 1/132.507$,
 $\alpha_s = 0.118$,
- $\Gamma_Z = 2.441404 \text{ GeV}$, $\Gamma_H = 6.382339 \text{ MeV}$.

The renormalization and factorization scale is set to $\sum M_i^T/2$, M_i^T are the transverse mass of all final state particles.

In our analysis, the total cross section in the SM including the aTGC is taken as[‡]

$$\sigma_{\text{Tot}} = \sigma_{mixed_2}^{\text{SM}} + (\sigma_{\text{NLO}}^{\text{aTGC}} - \sigma_{\text{NLO}}^{\text{SM}}),\tag{14}$$

the SM is considered at order $mixed_2$, whereas the aTGC contribution along with its interference with the SM are considered at NLO in QCD (as the NNLO contribution is not known with aTGC).

[‡] $mixed_1 \approx q\bar{q}(\mathcal{O}(\alpha_s)) + gg(\mathcal{O}(\alpha_s^2))$, $mixed_2 \approx q\bar{q}(\mathcal{O}(\alpha_s^2)) + gg(\mathcal{O}(\alpha_s^3))$

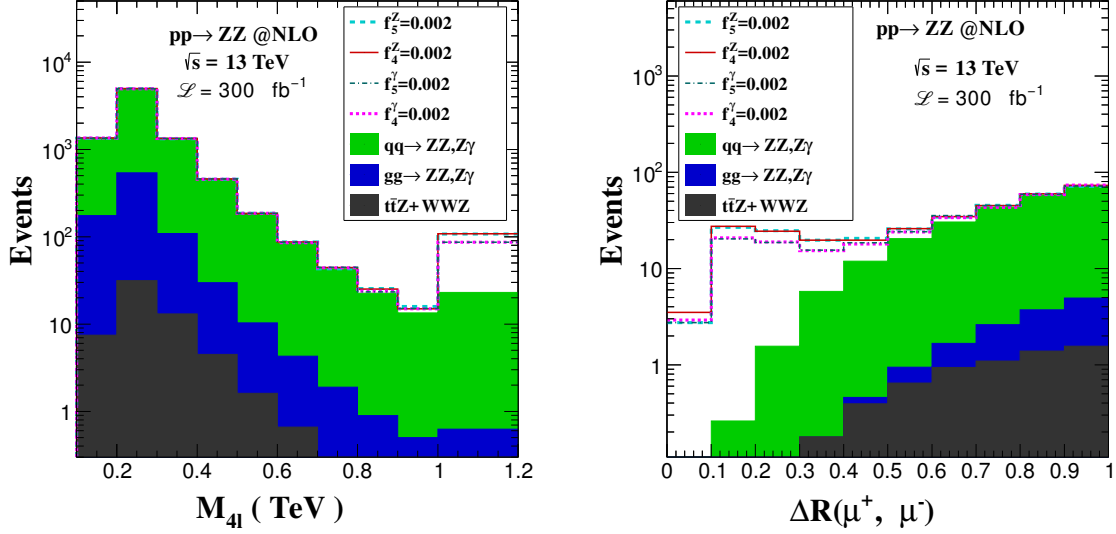


Figure 2: M_{4l} (*left-panel*) and ΔR between μ^+, μ^- (*right-panel*) distribution in ZZ production at the LHC at $\sqrt{s} = 13$ TeV and $\mathcal{L} = 300 \text{ fb}^{-1}$ at NLO in QCD. The SM signal and background are shown in shaded region, while aTGC contributions are shown with different line types.

We will use polarization asymmetries as described in the previous section in our analysis. Assuming that the NNLO effect cancels away because of the ratio of two cross section, we will use the asymmetries as

$$A_i = \frac{\Delta\sigma_i^{\text{mixed}_1}}{\sigma^{\text{mixed}_1}}. \quad (15)$$

We use total cross section at mixed_2 order and asymmetries at mixed_1 order to put constrain on the anomalous couplings. We note that the Z boson momenta is required to be reconstructed to obtain its polarization asymmetries, which require the right pairing of two oppositely charged leptons coming from a same Z boson in $4e/4\mu$ channel. The right paring of leptons for the Z boson in the same flavoured channel is possible with $\sim 95.5 \%$ for $M_{4l} > 300$ GeV and $\sim 99 \%$ for $M_{4l} > 700$ GeV for both SM and aTGC by requiring a smaller value of $|M_Z - M_{l+l-}|$. This small miss pairing is neglected as it allows to use the $2e2\mu$ channel as a proxy for the full $4l$ final state with good enough accuracy.

3.1 Effect of aTGC in distributions

The effect of aTGC on observables varies with energy scale. We study the effect of aTGC on various observables in their distribution and determine the signal region. In Fig. 2 we show four lepton invariant mass (M_{4l}) or centre-of-mass energy (\sqrt{s}) distribution (*left-panel*) and ΔR distribution of $\mu^+\mu^-$ pair (*right-panel*) at $\sqrt{s} = 13$ TeV for the SM along with background $t\bar{t}Z + WWZ$ and some benchmark aTGC points for events normalized to luminosity 300 fb^{-1} using MADANALYSIS5 [72]. The gg contribution is at its LO ($\mathcal{O}(\alpha_s^2)$), while all other contributions are shown at NLO ($\mathcal{O}(\alpha_s)$). The $q\bar{q} \rightarrow ZZ, Z\gamma$ contribution is shown in *green band*, $gg \rightarrow ZZ, Z\gamma$ is in *blue band* and the background $t\bar{t}Z + WWZ$ contribution is shown in *grey band*. The aTGC contribution for various choices are shown in *dashed/cyan* ($f_5^Z = 0.002$), *solid/red* ($f_4^Z = 0.002$), *dashed-dotted/dark-green* ($f_5^\gamma = 0.002$) and *small-dashed/magenta* ($f_4^\gamma = 0.002$). For the M_{4l} distribution in left, all events above 1 TeV are added in the last bin. All the aTGC benchmark

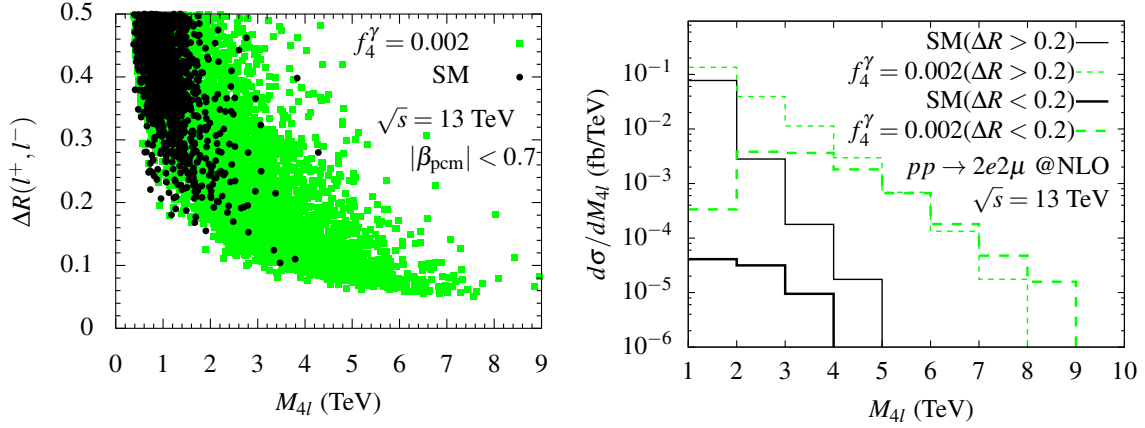


Figure 3: M_{4l} vs ΔR scattered plot (*left*) and M_{4l} distribution for $\Delta R(l^+, l^-) \geq 0.2$ (*right*) in ZZ production at the LHC at $\sqrt{s} = 13$ TeV for the SM and for aTGC with $f_4^\gamma = 0.002$.

i.e., $f_i^V = 0.002$ are not visibly different than the SM $q\bar{q}$ contribution upto $\sqrt{\hat{s}} = 0.8$ TeV and there are significant excess of events in the last bin, i.e., above $\sqrt{\hat{s}} = 1$ TeV. This is due to momentum dependence [22] of the interaction vertex that leads to increasing contribution at higher momentum transfer. In the distribution of $\Delta R(\mu^+, \mu^-)$ in the *right-panel*, the effect of aTGC is higher for lower ΔR (below 0.5). In the ZZ process, the Z bosons are highly boosted for larger $\sqrt{\hat{s}}$ and their decay products are collimated leading to a smaller ΔR separation between the decay leptons. To see this kinematic effect we plot events in $M_{4l} - \Delta R$ plane in Fig. 3 (*left-panel*). Here, we choose a minimum ΔR between e pair and μ pair event by event. We note that additional events coming from aTGC contributions have higher M_{4l} and lower ΔR between leptons. For $\Delta R < 0.2$ most of the events contribute to the $M_{4l} > 1$ TeV bin and they are dominantly coming from aTGC, Fig. 3 (*right-panel*). Thus we can choose $M_{4l} > 1$ TeV to be the signal region.

4 Sensitivity of observables and limits on the anomalous couplings

In this analysis, the set of observables consist of the cross section and polarization asymmetries \widetilde{A}_{xz} , $A_{x^2-y^2}$, and A_{zz} . The signal region for the cross section σ is chosen to be $M_{4l} > 1$ TeV as we have discussed in the previous section. In case of asymmetries, we choose the signal region as $M_{4l} > 0.3$ TeV for \widetilde{A}_{xz} and $M_{4l} > 0.7$ TeV for $A_{x^2-y^2}$ and A_{zz} as the effect of aTGC is found to be best in these region corresponding to these asymmetries. The expression for the cross section and the polarization asymmetries as a function of couplings are obtained by numerical fitting the data generated by MADGRAPH5_aMC@NLO. The events are generated for different set of values of the couplings $f_i^V = (f_4^\gamma, f_4^Z, f_5^\gamma, f_5^Z)$ and then various cross sections, i.e., the total cross section and the numerator of the asymmetries, \mathcal{O} , are fitted as

$$\mathcal{O} = \mathcal{O}_0 + f_i^V \times \mathcal{O}_i + f_i^V \times f_j^V \times \mathcal{O}_{ij}, \quad (16)$$

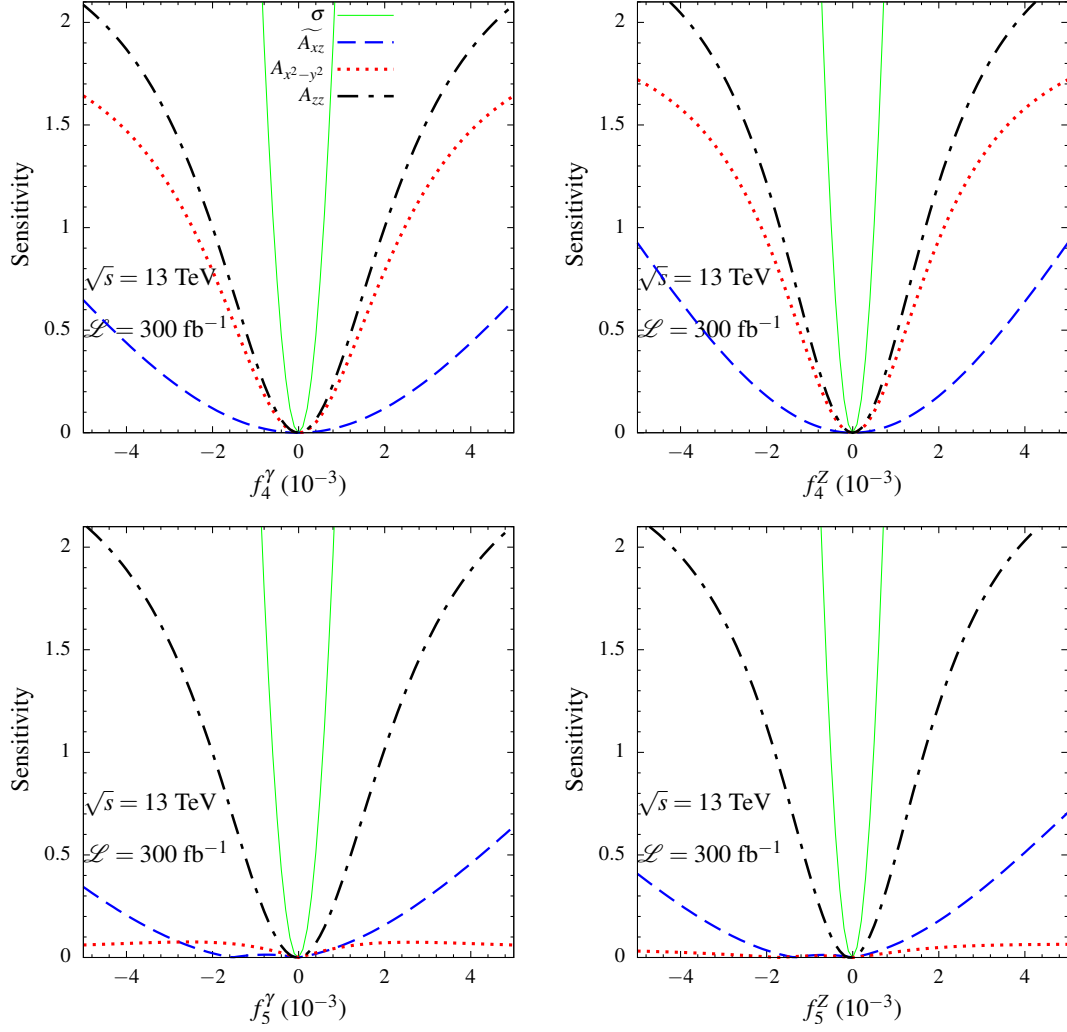


Figure 4: The sensitivity of the cross section and the polarization observables to the anomalous couplings at $\sqrt{s} = 13$ TeV and $\mathcal{L} = 300 \text{ fb}^{-1}$ in ZZ production at the LHC.

in general, where \mathcal{O}_0 is the value of corresponding cross sections in the SM. The observables, considered here, are all CP -even in nature which leads to the modification of Eq. (16) as

$$\mathcal{O} = \mathcal{O}_0 + f_5^V \times \mathcal{O}_5^V + f_4^\gamma f_4^Z \times \mathcal{O}_4^{\gamma,Z} + f_5^\gamma f_5^Z \times \mathcal{O}_5^{\gamma,Z} + (f_i^V)^2 \times \mathcal{O}_i^{VV}, \quad (17)$$

as the f_4^V are CP -odd, while f_5^V are CP -even couplings reducing the unknown from 15 to 9 to be solved. The numerical expressions of the cross section and the asymmetries as a function of the couplings are given in A. The observables are obtained up to $\mathcal{O}(\Lambda^{-4})$, i.e., quadratic in dimension-6. In practice, one should consider the effect of dimension-8 contribution at linear order. However, we choose to work with only dimension-6 in couplings with a contribution up to quadratic so as to compare the results with the current LHC constraints on dimension-6 parameters [42]. A note on keeping terms up to quadratic in couplings, and not terminating at linear order, is presented in B.

4.1 Sensitivity of observables to the couplings

The sensitivity of an observable $\mathcal{O}(f_i)$ to coupling f_i is defined as

$$\mathcal{SO}(f_i) = \frac{|\mathcal{O}(f_i) - \mathcal{O}(f_i = 0)|}{\delta\mathcal{O}}, \quad (18)$$

where $\delta\mathcal{O}$ is the estimated error in \mathcal{O} . For cross section and asymmetries, the errors are

$$\delta\sigma = \sqrt{\frac{\sigma}{\mathcal{L}} + (\epsilon_\sigma\sigma)^2} \quad \text{and} \quad \delta A_i = \sqrt{\frac{1 - A_i^2}{\mathcal{L} \times \sigma} + \epsilon_A^2}, \quad (19)$$

where \mathcal{L} is the integrated luminosity and ϵ_σ and ϵ_A are the systematic uncertainty for the cross section and the asymmetries, respectively. We consider $\epsilon_\sigma = 5\%$ [42] and $\epsilon_A = 2\%$ in this analysis as a benchmark. The sensitivity of all the observables to the couplings are shown in Fig. 4 for $\mathcal{L} = 300 \text{ fb}^{-1}$. We find asymmetries to be less sensitive than the cross section to the couplings and thus cross section wins in putting limits on the couplings. The sensitivity curve of all the couplings in each observable are symmetric about zero as f_4^V (being CP -odd) does not appear in linear in any observables and also the linear contribution from f_5^V are negligibly small compared to their quadratic contribution (see A). For example, the coefficient of f_5^V are ~ 1 in $\sigma(M_{4l} > 1 \text{ TeV})$ (Eq. (21)), while the coefficient of $(f_5^V)^2$ are $\sim 5 \times 10^4$. Thus even at $f_5^V = 10^{-3}$ the quadratic contribution is 50 times stronger than the linear one. Although the asymmetries are not strongly sensitive to the couplings as the cross section, they are useful in the measurement of the anomalous couplings, which will be discussed in the next section.

It is noteworthy to mention that the sensitivity of $A_{x^2-y^2}$ are flat and negligible for CP -even couplings f_5^V , while they vary significantly for CP -odd couplings f_4^V . Thus the asymmetry $A_{x^2-y^2}$, although a CP -even observables, is able to distinguish between CP -odd and CP -even interactions in the ZZ production at the LHC.

We use the total χ^2 as

$$\chi^2(f_i) = \sum_j [\mathcal{SO}_j(f_i)]^2 \quad (20)$$

to obtain the single parameter limits on the couplings by varying one parameter at a time and keeping all other to their SM values. The single parameter limits thus obtained on all the anomalous couplings at 95 % C.L. for four benchmark luminosities $\mathcal{L} = 35.9 \text{ fb}^{-1}$, 150 fb^{-1} , 300 fb^{-1} and 1000 fb^{-1} are presented in Table 2. The limit at $\mathcal{L} = 35.9 \text{ fb}^{-1}$ given in the first column of Table 2 are comparable to the tightest limit available at the LHC by CMS [65] given in Eq. (2).

Table 2: One parameter limits (10^{-3}) at 95 % C.L. on anomalous couplings in ZZ production at the LHC at $\sqrt{s} = 13$ TeV for various luminosities.

param / \mathcal{L}	35.9 fb $^{-1}$	150 fb $^{-1}$	300 fb $^{-1}$	1000 fb $^{-1}$
f_4^γ	+1.22 -1.20	+0.85 -0.85	+0.72 -0.72	+0.55 -0.55
f_5^γ	+1.21 -1.23	+0.84 -0.87	+0.71 -0.74	+0.54 -0.57
f_4^Z	+1.04 -1.03	+0.73 -0.72	+0.62 -0.61	+0.47 -0.47
f_5^Z	+1.03 -1.05	+0.72 -0.74	+0.61 -0.63	+0.46 -0.49

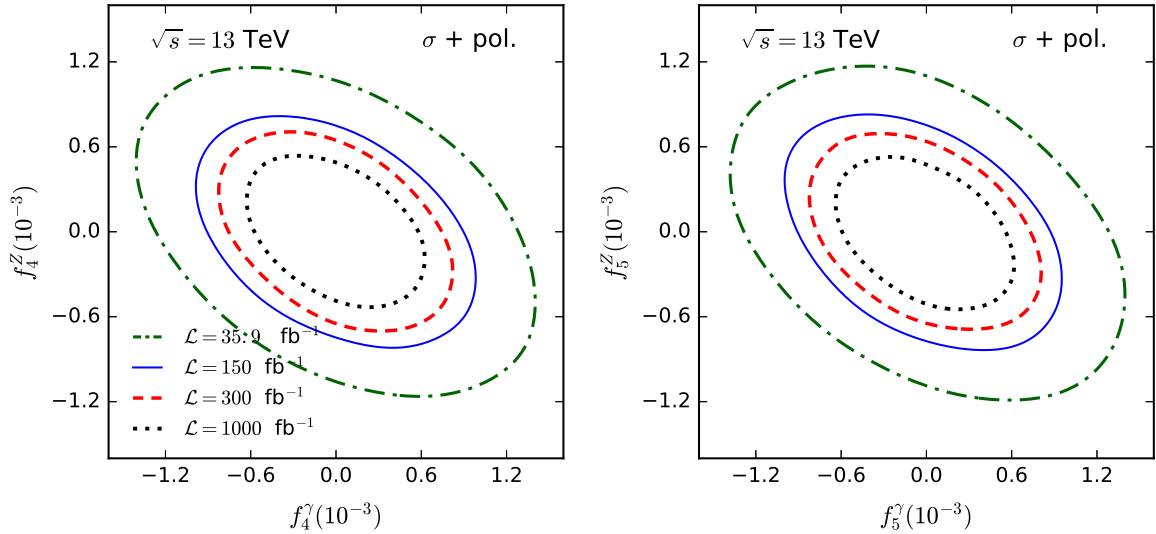


Figure 5: Two dimensional marginalised contours at 95 % BCI from MCMC using the cross section σ along with polarization asymmetries (pol.) at $\sqrt{s} = 13$ TeV for various luminosities in ZZ production at the LHC.

4.2 Limits on the couplings from MCMC

A likelihood-based analysis using the total χ^2 with the MCMC method is done by varying all the parameters simultaneously to extract simultaneous limits on all the anomalous couplings for the four benchmark luminosities chosen. The two dimensional marginalised contours at 95 % C.L. in the f_4^γ - f_4^Z and f_5^γ - f_5^Z planes are shown in Fig. 5 for the four benchmark luminosities chosen, using the cross section together with the polarization asymmetries, i.e, using $(\sigma + \text{pol.})$. The outer most contours are for $\mathcal{L} = 35.9 \text{ fb}^{-1}$ and the innermost contours are for $\mathcal{L} = 1000 \text{ fb}^{-1}$. The corresponding simultaneous limits on the aTGC couplings for four benchmark luminosities are presented in Table 3. The simultaneous limits are usually less tight than the one-dimensional limits, but find the opposite in some case, which can be seen comparing Table 3 with Table 2. The reason for this is the following. The cross section, the dominant observable, has a very little linear dependence, while it has a large quadratic dependence on the couplings (see Eq. (21)). As a result, when one obtains the limit on one parameter in the multi-parameter analysis, a slight deviation on any other parameter from zero (SM point) tightens the limit on the former coupling.

Table 3: Simultaneous limits (10^{-3}) at 95 % C.L. on anomalous couplings in ZZ production at the LHC at $\sqrt{s} = 13$ TeV for various luminosities from MCMC.

param / \mathcal{L}	35.9 fb $^{-1}$	150 fb $^{-1}$	300 fb $^{-1}$	1000 fb $^{-1}$
f_4^γ	+1.17 -1.15	+0.81 -0.81	+0.67 -0.68	+0.52 -0.52
f_5^γ	+1.50 -1.13	+0.78 -0.83	+0.66 -0.68	+0.51 -0.53
f_4^Z	+0.95 -0.96	+0.67 -0.67	+0.58 -0.58	+0.45 -0.44
f_5^Z	+0.95 -0.98	+0.68 -0.69	+0.57 -0.57	+0.43 -0.45

4.3 Role of polarization asymmetries in parameter extraction

The inclusion of polarization asymmetries with the cross section has no significant effect in constraining the anomalous couplings. The asymmetries may still be useful in extracting parameters if excess events were found at the LHC. To explore this, we do a toy analysis of parameter extraction using the data for all aTGC couplings $f_i^V = 0.002$ (well above current limit) and use the MCMC method to extract back these parameters. In Fig. 6, we show two-dimensional marginalized contours for the four benchmark luminosities for the benchmark aTGC couplings point $f_i^V = 0.002$ in f_4^γ - f_4^Z and f_5^γ - f_5^Z planes for the set of observables σ and $(\sigma + \text{pol.})$ for comparison. The *darker-shaded* regions are for 68 % C.L., while *lighter-shaded* regions are for 95 % C.L. The dot (\bullet) and the star (\star) mark in the plot are for the SM (0,0) and aTGC benchmark (0.002,0.002) points, respectively. We note that the SM point is inside the 68 % C.L. contours even at a high luminosity of $\mathcal{L} = 1000$ fb $^{-1}$ if we use only cross section as observable, see row-1 and 3 of Fig. 6. The distinction between the SM and the aTGC get improved when polarization asymmetries are included, i.e., the SM point is outside the 95 % C.L. contour for luminosity of much less than $\mathcal{L} = 1000$ fb $^{-1}$, see row-2 and 4 of the figure. As the luminosity increases, from the left column to the right, the contours for $(\sigma + \text{pol.})$ shrink around the star (\star) mark maintaining the shape of a ring giving better exclusion of the SM from aTGC benchmark. Polarization asymmetries are thus useful in the measurement of the anomalous couplings if excess events are found at the LHC.

5 Conclusions

In conclusion, we studied anomalous triple gauge boson couplings in the neutral sector in ZZ pair production at the LHC and investigated the role of Z boson polarizations. The QCD correction in this process is very high and can not be ignored. We obtained the cross section and the asymmetries at higher order in QCD. The aTGC contributes more in the higher \sqrt{s} region as they are momentum dependent. The major background $t\bar{t}Z + WWZ$ are negligibly small and they vanish in the signal regions. Although the asymmetries are not as sensitive as the cross section to the couplings, the asymmetry $A_{x^2-y^2}$ is able to distinguish between CP -even and CP -odd couplings. We estimate the one parameter as well as simultaneous limits on the couplings using all the observables based on the total χ^2 for luminosities 35.9 fb $^{-1}$, 150 fb $^{-1}$, 300 fb $^{-1}$ and 1000 fb $^{-1}$. Our one parameter limits are comparable to the best available limits obtained by the LHC [42]. The asymmetries are instrumental in extracting the parameters should a deviation from the SM is observed at the LHC. We did a toy analysis of parameter extraction with a

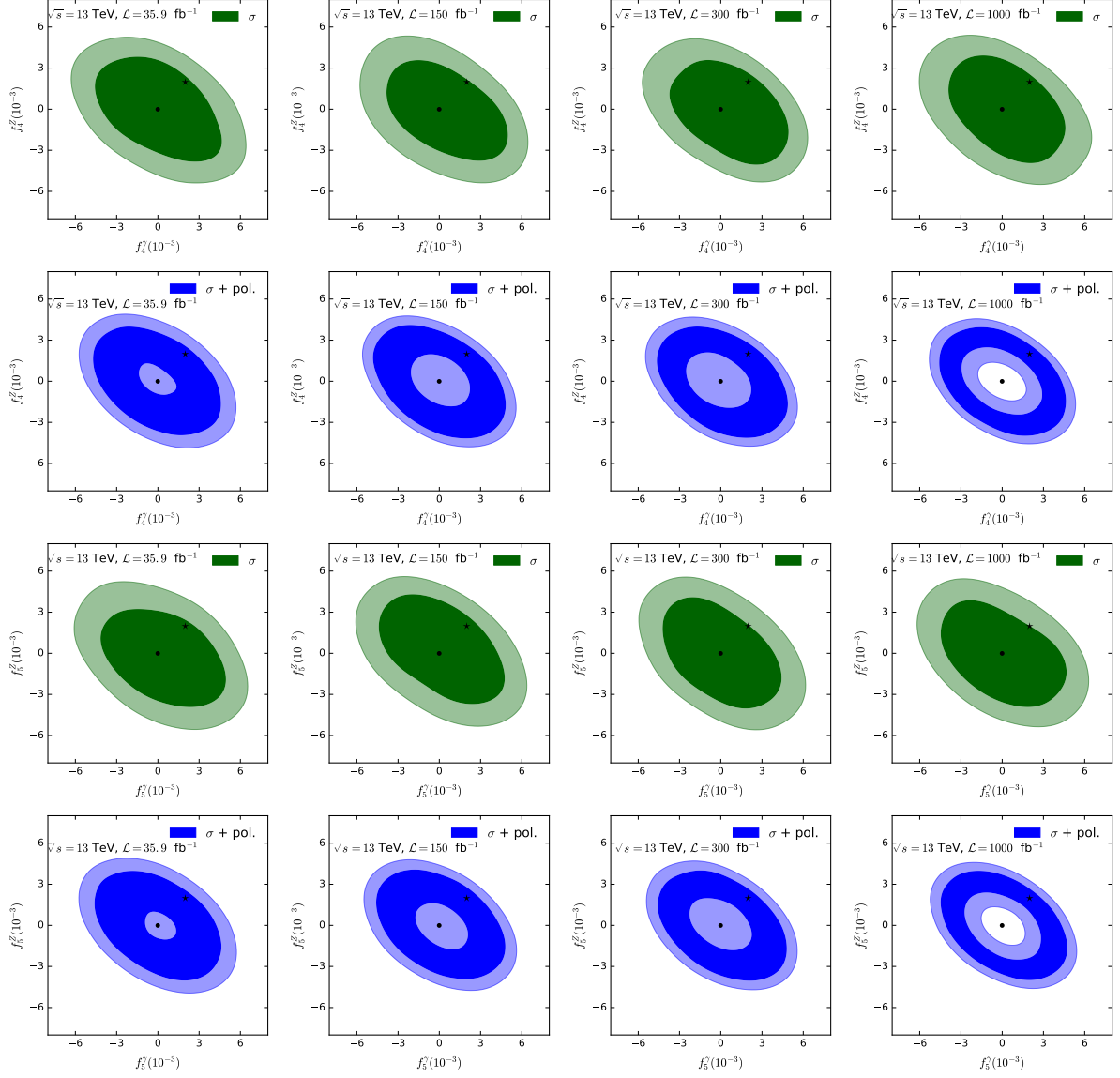


Figure 6: Comparison of σ vs $(\sigma + \text{pol.})$ in two dimensional marginalised contours from MCMC for aTGC benchmark $f_i^V = 0.002$ in f_4^γ - f_4^Z panel and f_5^γ - f_5^Z panel at $\sqrt{s} = 13$ TeV for various luminosities in ZZ production at the LHC.

benchmark aTGC coupling point with $f_i^V = 0.002$ and found that polarization with the cross section can exclude the SM from the aTGC point better than the cross section can do alone. In this work, the observables for the aTGC are obtained at $\mathcal{O}(\alpha_s)$, while they are obtained in the next order in the SM. The NNLO result in aTGC, when available, is expected to improve the limits on the couplings.

Acknowledgements: We thank Dr. Debajyoti Choudhury, Dr. V. Ravindran, Dr. Ayres Freitas and Dr. Adam Falkowski for fruitful discussion. R. R. thanks Department of Science and Technology, Government of India for support through DST-INSPIRE Fellowship for doctoral program, INSPIRE CODE IF140075, 2014.

Appendix A Expressions of observables

$$\begin{aligned}
\sigma(M_{4l} > 1 \text{ TeV}) &= 0.096685 + f_5^\gamma \times 1.9492 + f_5^Z \times 1.7106 \\
&+ f_4^\gamma f_4^Z \times 51788 + f_5^\gamma f_5^Z \times 51204 + (f_4^\gamma)^2 \times 54933 \\
&+ (f_4^Z)^2 \times 75432 + (f_5^\gamma)^2 \times 54507 + (f_5^Z)^2 \times 74466 \text{ fb}
\end{aligned} \tag{21}$$

$$\begin{aligned}
\sigma(M_{4l} > 0.3 \text{ TeV}) &= 7.9503 + f_5^\gamma \times 16.886 + f_5^Z \times 4.0609 \\
&+ f_4^\gamma f_4^Z \times 58561 + f_5^\gamma f_5^Z \times 54131 + (f_4^\gamma)^2 \times 58771 \\
&+ (f_4^Z)^2 \times 81647 + (f_5^\gamma)^2 \times 55210 + (f_5^Z)^2 \times 78325 \text{ fb}
\end{aligned} \tag{22}$$

$$\begin{aligned}
\sigma(M_{4l} > 0.7 \text{ TeV}) &= 0.37616 + f_5^\gamma \times 3.8161 + f_5^Z \times 2.9704 \\
&+ f_4^\gamma f_4^Z \times 55005 + f_5^\gamma f_5^Z \times 52706 + (f_4^\gamma)^2 \times 57982 \\
&+ (f_4^Z)^2 \times 80035 + (f_5^\gamma)^2 \times 57131 + (f_5^Z)^2 \times 78515 \text{ fb}
\end{aligned} \tag{23}$$

$$\begin{aligned}
\widetilde{A_{xz}^{\text{num.}}}(M_{4l} > 0.3 \text{ TeV}) &= -0.77152 + f_5^\gamma \times 6.1912 + f_5^Z \times 7.8270 \\
&+ f_4^\gamma f_4^Z \times 2869.5 + f_5^\gamma f_5^Z \times 396.94 + (f_4^\gamma)^2 \times 1029.7 \\
&+ (f_4^Z)^2 \times 2298.7 - (f_5^\gamma)^2 \times 274.02 \\
&- (f_5^Z)^2 \times 1495.5 \text{ fb}
\end{aligned} \tag{24}$$

$$\begin{aligned}
A_{x^2-y^2}^{\text{num.}}(M_{4l} > 0.7 \text{ TeV}) &= -0.04295 + f_5^\gamma \times 1.5563 + f_5^Z \times 0.37094 \\
&+ f_4^\gamma f_4^Z \times 3299.8 - f_5^\gamma f_5^Z \times 5853.9 + (f_4^\gamma)^2 \times 4241.8 \\
&+ (f_4^Z)^2 \times 5679.3 - (f_5^\gamma)^2 \times 6520.1 \\
&- (f_5^Z)^2 \times 8559.3 \text{ fb}
\end{aligned} \tag{25}$$

$$\begin{aligned}
A_{zz}^{\text{num.}}(M_{4l} > 0.7 \text{ TeV}) &= 0.048175 - f_5^\gamma \times 0.12125 - f_5^Z \times 1.5339 \\
&- f_4^\gamma f_4^Z \times 6449.2 - f_5^\gamma f_5^Z \times 5860.4 - (f_4^\gamma)^2 \times 6344.7 \\
&- (f_4^Z)^2 \times 8907.4 - (f_5^\gamma)^2 \times 6457.7 \\
&- (f_5^Z)^2 \times 8346.8 \text{ fb}
\end{aligned} \tag{26}$$

The asymmetries will be given as,

$$\begin{aligned}\widetilde{A}_{xz} &= \frac{\widetilde{A_{xz}^{\text{num.}}}(M_{4l} > 0.3 \text{ TeV})}{\sigma(M_{4l} > 0.3 \text{ TeV})}, \\ A_{x^2-y^2} &= \frac{A_{x^2-y^2}^{\text{num.}}(M_{4l} > 0.7 \text{ TeV})}{\sigma(M_{4l} > 0.7 \text{ TeV})}, \\ A_{zz} &= \frac{A_{zz}^{\text{num.}}(M_{4l} > 0.7 \text{ TeV})}{\sigma(M_{4l} > 0.7 \text{ TeV})}.\end{aligned}\tag{27}$$

Appendix B Note on linear approximation

We note that, the linear approximation of considering anomalous couplings will be valid if the quadratic contribution on the cross section will be much smaller than the linear contribution, i.e.,

$$|f_i \times \sigma_i| \gg |f_i^2 \times \sigma_{ii}|, \quad \text{or} \quad |f_i| \ll \frac{\sigma_i}{\sigma_{ii}},\tag{28}$$

where σ_i and σ_{ii} are the linear and quadratic coefficient of the coupling f_i in the cross section. Based on $\sigma(M_{4l} > 1 \text{ TeV})$ in Eq. (21) the linear approximation constrain f_5^V as

$$|f_5^Z| \ll 2.2 \times 10^{-5}, \quad |f_5^\gamma| \ll 3.5 \times 10^{-5},\tag{29}$$

which are much much smaller than the limit (see Eq. (2)) observed at the LHC [42]. To this end we keep terms upto quadratic in couplings in our analysis.

References

- [1] **CMS** Collaboration, S. Chatrchyan *et al.*, Observation of a new boson at a mass of 125 GeV with the CMS experiment at the LHC, *Phys. Lett.* **B716** (2012) 30–61, [arXiv:1207.7235 \[hep-ex\]](#).
- [2] F. Larios, M. A. Perez, G. Tavares-Velasco, and J. J. Toscano, Trilinear neutral gauge boson couplings in effective theories, *Phys. Rev.* **D63** (2001) 113014, [arXiv:hep-ph/0012180 \[hep-ph\]](#).
- [3] O. Cata, Revisiting ZZ and γZ production with effective field theories, [arXiv:1304.1008 \[hep-ph\]](#).
- [4] C. Degrande, A basis of dimension-eight operators for anomalous neutral triple gauge boson interactions, *JHEP* **02** (2014) 101, [arXiv:1308.6323 \[hep-ph\]](#).
- [5] K. Hagiwara, R. D. Peccei, D. Zeppenfeld, and K. Hikasa, Probing the Weak Boson Sector in $e^+e^- \rightarrow W^+W^-$, *Nucl. Phys.* **B282** (1987) 253–307.
- [6] G. J. Gounaris, J. Layssac, and F. M. Renard, Signatures of the anomalous $Z\gamma$ and ZZ production at the lepton and hadron colliders, *Phys. Rev.* **D61** (2000) 073013, [arXiv:hep-ph/9910395 \[hep-ph\]](#).
- [7] H. Czyz, K. Kolodziej, and M. Zralek, Composite Z Boson and CP Violation in the Process $e^+e^- \rightarrow Z\gamma$, *Z. Phys.* **C43** (1989) 97.

- [8] U. Baur and E. L. Berger, Probing the weak boson sector in $Z\gamma$ production at hadron colliders, *Phys. Rev.* **D47** (1993) 4889–4904.
- [9] D. Choudhury and S. D. Rindani, Test of CP violating neutral gauge boson vertices in $e^+e^- \rightarrow \gamma Z$, *Phys. Lett.* **B335** (1994) 198–204, [arXiv:hep-ph/9405242](#) [hep-ph].
- [10] S. Y. Choi, Probing the weak boson sector in $\gamma e \rightarrow Ze$, *Z. Phys.* **C68** (1995) 163–172, [arXiv:hep-ph/9412300](#) [hep-ph].
- [11] H. Aihara *et al.*, Anomalous gauge boson interactions, *World scientific: Advanced Series on Directions in High Energy Physics / Electroweak Symmetry Breaking and New Physics at the TeV Scale* (1997) 488–547, [arXiv:hep-ph/9503425](#) [hep-ph].
- [12] J. Ellison and J. Wudka, Study of trilinear gauge boson couplings at the Tevatron collider, *Ann. Rev. Nucl. Part. Sci.* **48** (1998) 33–80, [arXiv:hep-ph/9804322](#) [hep-ph].
- [13] G. J. Gounaris, J. Layssac, and F. M. Renard, Off-shell structure of the anomalous Z and γ selfcouplings, *Phys. Rev.* **D65** (2002) 017302, [arXiv:hep-ph/0005269](#) [hep-ph]. [Phys. Rev.D62,073012(2000)].
- [14] U. Baur and D. L. Rainwater, Probing neutral gauge boson selfinteractions in ZZ production at hadron colliders, *Phys. Rev.* **D62** (2000) 113011, [arXiv:hep-ph/0008063](#) [hep-ph].
- [15] T. G. Rizzo, Polarization asymmetries in gamma e collisions and triple gauge boson couplings revisited, in *Physics and experiments with future linear e^+e^- colliders. Proceedings, 4th Workshop, LCWS'99, Sitges, Spain, April 28-May 5, 1999. Vol. 1: Physics at linear colliders*, pp. 529–533. 1999. [arXiv:hep-ph/9907395](#) [hep-ph]. <http://www-public.slac.stanford.edu/sciDoc/docMeta.aspx?slacPubNumber=SLAC-PUB-8192>.
- [16] S. Atag and I. Sahin, ZZ gamma and Z gamma gamma couplings in gamma e collision with polarized beams, *Phys. Rev.* **D68** (2003) 093014, [arXiv:hep-ph/0310047](#) [hep-ph].
- [17] B. Ananthanarayan, S. D. Rindani, R. K. Singh, and A. Bartl, Transverse beam polarization and CP-violating triple-gauge-boson couplings in $e^+e^- \rightarrow \gamma Z$, *Phys. Lett.* **B593** (2004) 95–104, [arXiv:hep-ph/0404106](#) [hep-ph]. [Erratum: Phys. Lett.B608,274(2005)].
- [18] B. Ananthanarayan, S. K. Garg, M. Patra, and S. D. Rindani, Isolating CP-violating γZZ coupling in $e^+e^- \rightarrow \gamma Z$ with transverse beam polarizations, *Phys. Rev.* **D85** (2012) 034006, [arXiv:1104.3645](#) [hep-ph].
- [19] B. Ananthanarayan, J. Lahiri, M. Patra, and S. D. Rindani, New physics in $e^+e^- \rightarrow Z\gamma$ at the ILC with polarized beams: explorations beyond conventional anomalous triple gauge boson couplings, *JHEP* **08** (2014) 124, [arXiv:1404.4845](#) [hep-ph].
- [20] P. Poulou and S. D. Rindani, CP violating $Z\gamma\gamma$ and top quark electric dipole couplings in $\gamma\gamma \rightarrow t\bar{t}$, *Phys. Lett.* **B452** (1999) 347–354, [arXiv:hep-ph/9809203](#) [hep-ph].
- [21] A. Senol, $ZZ\gamma$ and $Z\gamma\gamma$ anomalous couplings in γp collision at the LHC, *Phys. Rev.* **D87** (2013) 073003, [arXiv:1301.6914](#) [hep-ph].

- [22] R. Rahaman and R. K. Singh, On polarization parameters of spin-1 particles and anomalous couplings in $e^+e^- \rightarrow ZZ/Z\gamma$, *Eur. Phys. J.* **C76** no. 10, (2016) 539, [arXiv:1604.06677 \[hep-ph\]](#).
- [23] R. Rahaman and R. K. Singh, On the choice of beam polarization in $e^+e^- \rightarrow ZZ/Z\gamma$ and anomalous triple gauge-boson couplings, *Eur. Phys. J.* **C77** no. 8, (2017) 521, [arXiv:1703.06437 \[hep-ph\]](#).
- [24] I. Ots, H. Uiho, H. Liivat, R. Saar, and R. K. Loide, Possible anomalous Z Z gamma and Z gamma gamma couplings and Z boson spin orientation in $e^+e^- \rightarrow Z\gamma$: The role of transverse polarization, *Nucl. Phys.* **B740** (2006) 212–221.
- [25] B. Ananthanarayan and S. D. Rindani, CP violation at a linear collider with transverse polarization, *Phys. Rev.* **D70** (2004) 036005, [arXiv:hep-ph/0309260 \[hep-ph\]](#).
- [26] M. Chiesa, A. Denner, and J.-N. Lang, Anomalous triple-gauge-boson interactions in vector-boson pair production with RECOLA2, *Eur. Phys. J.* **C78** no. 6, (2018) 467, [arXiv:1804.01477 \[hep-ph\]](#).
- [27] M. Chiesa, A. Denner, and J.-N. Lang, Effects of anomalous triple-gauge-boson interactions in diboson production with RECOLA2, in *14th DESY Workshop on Elementary Particle Physics: Loops and Legs in Quantum Field Theory 2018 (LL2018) St Goar, Germany, April 29-May 4, 2018*. 2018. [arXiv:1808.03167 \[hep-ph\]](#).
- [28] **L3** Collaboration, M. Acciarri *et al.*, Search for anomalous $ZZ\gamma$ and $Z\gamma\gamma$ couplings in the process $e^+e^- \rightarrow Z\gamma$ at LEP, *Phys. Lett.* **B489** (2000) 55–64, [arXiv:hep-ex/0005024 \[hep-ex\]](#).
- [29] **OPAL** Collaboration, G. Abbiendi *et al.*, Search for trilinear neutral gauge boson couplings in $Z\gamma$ production at $\sqrt{s} = 189$ GeV at LEP, *Eur. Phys. J.* **C17** (2000) 553–566, [arXiv:hep-ex/0007016 \[hep-ex\]](#).
- [30] **OPAL** Collaboration, G. Abbiendi *et al.*, Study of Z pair production and anomalous couplings in e^+e^- collisions at \sqrt{s} between 190-GeV and 209-GeV, *Eur. Phys. J.* **C32** (2003) 303–322, [arXiv:hep-ex/0310013 \[hep-ex\]](#).
- [31] **L3** Collaboration, P. Achard *et al.*, Study of the $e^+e^- \rightarrow Z\gamma$ process at LEP and limits on triple neutral-gauge-boson couplings, *Phys. Lett.* **B597** (2004) 119–130, [arXiv:hep-ex/0407012 \[hep-ex\]](#).
- [32] **DELPHI** Collaboration, J. Abdallah *et al.*, Study of triple-gauge-boson couplings ZZZ, ZZgamma and Zgamma gamma LEP, *Eur. Phys. J.* **C51** (2007) 525–542, [arXiv:0706.2741 \[hep-ex\]](#).
- [33] **D0** Collaboration, V. M. Abazov *et al.*, Search for ZZ and $Z\gamma^*$ production in $p\bar{p}$ collisions at $\sqrt{s} = 1.96$ TeV and limits on anomalous ZZZ and $ZZ\gamma^*$ couplings, *Phys. Rev. Lett.* **100** (2008) 131801, [arXiv:0712.0599 \[hep-ex\]](#).
- [34] **CDF** Collaboration, T. Aaltonen *et al.*, Limits on Anomalous Trilinear Gauge Couplings in $Z\gamma$ Events from $p\bar{p}$ Collisions at $\sqrt{s} = 1.96$ TeV, *Phys. Rev. Lett.* **107** (2011) 051802, [arXiv:1103.2990 \[hep-ex\]](#).

- [35] **D0** Collaboration, V. M. Abazov *et al.*, $Z\gamma$ production and limits on anomalous $ZZ\gamma$ and $Z\gamma\gamma$ couplings in $p\bar{p}$ collisions at $\sqrt{s} = 1.96$ TeV, *Phys. Rev.* **D85** (2012) 052001, [arXiv:1111.3684 \[hep-ex\]](#).
- [36] **CMS** Collaboration, S. Chatrchyan *et al.*, Measurement of the ZZ production cross section and search for anomalous couplings in 2 l2l' final states in pp collisions at $\sqrt{s} = 7$ TeV, *JHEP* **01** (2013) 063, [arXiv:1211.4890 \[hep-ex\]](#).
- [37] **CMS** Collaboration, S. Chatrchyan *et al.*, Measurement of the production cross section for $Z\gamma \rightarrow \nu\bar{\nu}\gamma$ in pp collisions at $\sqrt{s} = 7$ TeV and limits on $ZZ\gamma$ and $Z\gamma\gamma$ triple gauge boson couplings, *JHEP* **10** (2013) 164, [arXiv:1309.1117 \[hep-ex\]](#).
- [38] **ATLAS** Collaboration, G. Aad *et al.*, Measurements of $W\gamma$ and $Z\gamma$ production in pp collisions at $\sqrt{s}=7$ TeV with the ATLAS detector at the LHC, *Phys. Rev.* **D87** no. 11, (2013) 112003, [arXiv:1302.1283 \[hep-ex\]](#). [Erratum: Phys. Rev.D91,no.11,119901(2015)].
- [39] **CMS** Collaboration, V. Khachatryan *et al.*, Measurement of the $Z\gamma$ Production Cross Section in pp Collisions at 8 TeV and Search for Anomalous Triple Gauge Boson Couplings, *JHEP* **04** (2015) 164, [arXiv:1502.05664 \[hep-ex\]](#).
- [40] **CMS** Collaboration, V. Khachatryan *et al.*, Measurement of the $Z\gamma \rightarrow \nu\bar{\nu}\gamma$ production cross section in pp collisions at $\sqrt{s} = 8$ TeV and limits on anomalous $ZZ\gamma$ and $Z\gamma\gamma$ trilinear gauge boson couplings, *Phys. Lett.* **B760** (2016) 448–468, [arXiv:1602.07152 \[hep-ex\]](#).
- [41] **ATLAS** Collaboration, M. Aaboud *et al.*, $ZZ \rightarrow \ell^+\ell^-\ell'^+\ell'^-$ cross-section measurements and search for anomalous triple gauge couplings in 13 TeV pp collisions with the ATLAS detector, *Phys. Rev.* **D97** no. 3, (2018) 032005, [arXiv:1709.07703 \[hep-ex\]](#).
- [42] **CMS** Collaboration, A. M. Sirunyan *et al.*, Measurements of the $pp \rightarrow ZZ$ production cross section and the $Z \rightarrow 4\ell$ branching fraction, and constraints on anomalous triple gauge couplings at $\sqrt{s} = 13$ TeV, *Eur. Phys. J.* **C78** (2018) 165, [arXiv:1709.08601 \[hep-ex\]](#). [Erratum: Eur. Phys. J.C78,no.6,515(2018)].
- [43] T. Corbett, M. J. Dolan, C. Englert, and K. Nordström, Anomalous neutral gauge boson interactions and simplified models, *Phys. Rev.* **D97** no. 11, (2018) 115040, [arXiv:1710.07530 \[hep-ph\]](#).
- [44] G. J. Gounaris, J. Layssac, and F. M. Renard, New and standard physics contributions to anomalous Z and gamma selfcouplings, *Phys. Rev.* **D62** (2000) 073013, [arXiv:hep-ph/0003143 \[hep-ph\]](#).
- [45] D. Choudhury, S. Dutta, S. Rakshit, and S. Rindani, Trilinear neutral gauge boson couplings, *Int. J. Mod. Phys.* **A16** (2001) 4891–4910, [arXiv:hep-ph/0011205 \[hep-ph\]](#).
- [46] S. Dutta, A. Goyal, and Mamta, New Physics Contribution to Neutral Trilinear Gauge Boson Couplings, *Eur. Phys. J.* **C63** (2009) 305–315, [arXiv:0901.0260 \[hep-ph\]](#).
- [47] B. Grzadkowski, O. M. Ogreid, and P. Osland, CP-Violation in the ZZZ and ZWW vertices at e^+e^- colliders in Two-Higgs-Doublet Models, *JHEP* **05** (2016) 025, [arXiv:1603.01388 \[hep-ph\]](#). [Erratum: JHEP11,002(2017)].

- [48] H. Bélusca-Maïto, A. Falkowski, D. Fontes, J. C. Romão, and J. P. Silva, CP violation in 2HDM and EFT: the ZZZ vertex, *JHEP* **04** (2018) 002, [arXiv:1710.05563 \[hep-ph\]](#).
- [49] N. G. Deshpande and X.-G. He, Triple neutral gauge boson couplings in noncommutative standard model, *Phys. Lett. B* **533** (2002) 116–120, [arXiv:hep-ph/0112320 \[hep-ph\]](#).
- [50] A. Senol, M. Köksal, and S. C. İnan, Probe of the Anomalous Quartic Couplings with Beam Polarization at the CLIC, *Adv. High Energy Phys.* **2017** (2017) 6970587, [arXiv:1603.01065 \[hep-ph\]](#).
- [51] Y. Wen, H. Qu, D. Yang, Q.-s. Yan, Q. Li, and Y. Mao, Probing triple-W production and anomalous WWWW coupling at the CERN LHC and future $\mathcal{O}(100)$ TeV proton-proton collider, *JHEP* **03** (2015) 025, [arXiv:1407.4922 \[hep-ph\]](#).
- [52] G. Perez, M. Sekulla, and D. Zeppenfeld, Anomalous quartic gauge couplings and unitarization for the vector boson scattering process $pp \rightarrow W^+W^+jjX \rightarrow \ell^+\nu_\ell\ell^+\nu_\ell jjX$, *Eur. Phys. J. C* **78** no. 9, (2018) 759, [arXiv:1807.02707 \[hep-ph\]](#).
- [53] F. Boudjema and R. K. Singh, A Model independent spin analysis of fundamental particles using azimuthal asymmetries, *JHEP* **07** (2009) 028, [arXiv:0903.4705 \[hep-ph\]](#).
- [54] J. A. Aguilar-Saavedra and J. Bernabeu, Breaking down the entire W boson spin observables from its decay, *Phys. Rev. D* **93** no. 1, (2016) 011301, [arXiv:1508.04592 \[hep-ph\]](#).
- [55] **OPAL** Collaboration, G. Abbiendi *et al.*, Measurement of W boson polarizations and CP violating triple gauge couplings from W^+W^- production at LEP, *Eur. Phys. J. C* **19** (2001) 229–240, [arXiv:hep-ex/0009021 \[hep-ex\]](#).
- [56] R. Rahaman and R. K. Singh, Constraining anomalous gauge boson couplings in $e^+e^- \rightarrow W^+W^-$ using polarization asymmetries with polarized beams, [arXiv:1711.04551 \[hep-ph\]](#).
- [57] J. Nakamura, Polarisation of the Z and W bosons in the processes $pp \rightarrow ZH$ and $pp \rightarrow W^\pm H$, *JHEP* **08** (2017) 008, [arXiv:1706.01816 \[hep-ph\]](#).
- [58] K. Rao and S. D. Rindani, W boson polarization as a measure of gauge-Higgs anomalous couplings at the LHC, *Nucl. Phys. B* **940** (2019) 78–87, [arXiv:1805.06602 \[hep-ph\]](#).
- [59] F. M. Renard, Polarization effects due to dark matter interaction between massive standard particles, [arXiv:1802.10313 \[hep-ph\]](#).
- [60] F. M. Renard, Z Polarization in $e^+e^- \rightarrow t\bar{t}Z$ for testing the top quark mass structure and the presence of final interactions, [arXiv:1803.10466 \[hep-ph\]](#).
- [61] F. M. Renard, W polarization in e^+e^- , gluon-gluon and $\gamma\gamma \rightarrow Wt\bar{b}$ for testing the top quark mass structure and the presence of final interactions, [arXiv:1807.00621 \[hep-ph\]](#).
- [62] F. M. Renard, Further tests of special interactions of massive particles from the Z polarization rate in $e^+e^- \rightarrow Zt\bar{t}$ and in $e^+e^- \rightarrow ZW^+W^-$, [arXiv:1808.05429 \[hep-ph\]](#).
- [63] F. M. Renard, Z polarization in $e^+e^- \rightarrow ZWW$ for testing special interactions of massive particles, [arXiv:1807.08938 \[hep-ph\]](#).

- [64] J. A. Aguilar-Saavedra, J. Bernabéu, V. A. Mitsou, and A. Segarra, The Z boson spin observables as messengers of new physics, *Eur. Phys. J.* **C77** no. 4, (2017) 234, [arXiv:1701.03115 \[hep-ph\]](#).
- [65] G. Heinrich, S. Jahn, S. P. Jones, M. Kerner, and J. Pires, NNLO predictions for Z-boson pair production at the LHC, *JHEP* **03** (2018) 142, [arXiv:1710.06294 \[hep-ph\]](#).
- [66] F. Cascioli, T. Gehrmann, M. Grazzini, S. Kallweit, P. Maierhöfer, A. von Manteuffel, S. Pozzorini, D. Rathlev, L. Tancredi, and E. Weihs, ZZ production at hadron colliders in NNLO QCD, *Phys. Lett.* **B735** (2014) 311–313, [arXiv:1405.2219 \[hep-ph\]](#).
- [67] J. Alwall, R. Frederix, S. Frixione, V. Hirschi, F. Maltoni, O. Mattelaer, H. S. Shao, T. Stelzer, P. Torrielli, and M. Zaro, The automated computation of tree-level and next-to-leading order differential cross sections, and their matching to parton shower simulations, *JHEP* **07** (2014) 079, [arXiv:1405.0301 \[hep-ph\]](#).
- [68] C. Bourrely, J. Soffer, and E. Leader, Polarization Phenomena in Hadronic Reactions, *Phys. Rept.* **59** (1980) 95–297.
- [69] V. Arunprasath, R. M. Godbole, and R. K. Singh, Polarization of a top quark produced in the decay of a gluino or a stop in an arbitrary frame, *Phys. Rev.* **D95** no. 7, (2017) 076012, [arXiv:1612.03803 \[hep-ph\]](#).
- [70] A. Velusamy and R. K. Singh, Polarization of a vector boson produced in decay of a heavy fermion in an arbitrary frame, *Phys. Rev.* **D98** no. 5, (2018) 053009, [arXiv:1805.00876 \[hep-ph\]](#).
- [71] F. Caola, K. Melnikov, R. Röntsch, and L. Tancredi, QCD corrections to ZZ production in gluon fusion at the LHC, *Phys. Rev.* **D92** no. 9, (2015) 094028, [arXiv:1509.06734 \[hep-ph\]](#).
- [72] E. Conte, B. Fuks, and G. Serret, MadAnalysis 5, A User-Friendly Framework for Collider Phenomenology, *Comput. Phys. Commun.* **184** (2013) 222–256, [arXiv:1206.1599 \[hep-ph\]](#).